# Multi-objective conditioning of a SVAT model for heat and $CO_2$ fluxes prediction

**XINGGUO MO**[1], **SUXIA LIU**[2], **ZHONGHUI LIN**[1], **XIAOMIN SUN**[1] **& ZHILIN ZHU**[1]

1 *Key Lab of Ecological Net Observation and Modelling,*
*Institute of Geographical Sciences and Natural Resources Research,*
*Chinese Academy of Sciences, Beijing 100101, China*
moxg@igsnrr.ac.cn

2 *Key Lab of Water Cycle and Related Land Surface Processes,*
*Institute of Geographical Sciences and Natural Resources Research,*
*Chinese Academy of Sciences, Beijing 100101, China*

**Abstract** The parameters of a SVAT model (VIP) are explored by a multi-objective likelihood measure using the Generalized Likelihood Uncertainty Estimation (GLUE) framework based on field data collected in the North China Plain during the winter wheat growing season in 2001. Agreement indexes of latent, sensible, ground heat and $CO_2$ fluxes and radiometric surface temperature between the observed and the modelled data are used to evaluate the model performance, in which 13 parameters were selected for calibration and model uncertainty estimation. Although the single objective approach effectively constrains the corresponding model response, the multiple objective technique, including both fluxes and state variables, presents a more efficient constraint. The outstanding effect of surface radiometric temperature for calibration suggests that thermal remote sensing might be a promising tool for distributed SVAT model calibration and evaluation over large areas. It is found that, although the model appears to have a serious equifinality problem, the interactions and compensation effects between the parameters are not strong, with both linear and nonlinear correlation coefficients being small. Sensitivity analyses using both scatter plots and partial correlation coefficients show that model responses are sensitive to half of 13 parameters.

**Key words** GLUE; parameter calibration; SVAT model; uncertainty

## INTRODUCTION

The increased atmospheric $CO_2$ concentration and induced global warming are expected to seriously affect many aspects of terrestrial ecosystems through the rate and magnitude of change in climate means and extremes. The changes in the ecosystems in turn will significantly influence the climate through their effects on the partitioning of energy into latent and sensible heat fluxes, as well as carbon fluxes on the land surface. Physical modelling of Soil–Vegetation–Atmosphere Transfer (SVAT) processes is an indispensable tool for study of these interactions between atmospheric $CO_2$, climate, land use, and terrestrial carbon pools and to predict ecosystem effects under different scenarios.

SVAT models are designed to predict a range of land surface fluxes (e.g. energy fluxes, carbon flux, runoff, evapotranspiration) and surface states (e.g. surface temperature, soil moisture), most of which are measurable at both the patch scale and the regional scale by tower instruments and remote sensing, respectively. However, since the limited data available for calibration may deteriorate the parameter robustness, SVAT models are generally deemed overparameterization. By adjusting the parameter values to achieve an acceptable match with observations, many distinct parameter sets over a wide range of parameter space can simulate behavioural fits, resulting in so-called equifinality (Beven & Binley, 1992) and giving rise to significant prediction uncertainty. The uncertainty of SVAT models may stem from model structure, scale inconsistency and boundary conditions. To reduce parameter uncertainty, model parameter calibration is necessary. Usually a single criterion is difficult to constrain the multiple model output variables (Gupta *et al*., 1999). As an alternative, the SVAT model should theoretically apply as more observed variables as possible to constrain the equifinality problem via the framework of multi-objective methodology.

With recent investigations on various aspects of SVAT processes (Avissar, 1998), there have been many documented studies to analyse the model uncertainties through both the single and multi-criterion for various kinds of SVAT models (Franks & Beven, 1998; Grieb *et al*., 1999; Gupta *et al*., 1999; Mo & Beven, 2004). Since different SVAT models have their own special treatments of land surface processes, it is certain that with different parameters involved, the model uncertainty performances vary. It is therefore scientifically meaningful to identify the parameter uncertainty for each of the SVAT models, in order to assess the model confidence, to improve the parameterization schemes and find some common features in the model uncertainty if they exist.

In this paper, parameter calibration and uncertainty analysis is carried out based on a SVAT model, known as VIP (Vegetation Interface Process model), originated from Mo & Liu (2001) and Mo & Beven (2004). The distinguishing characteristics of the model are the solution of the energy balance equations and the stomatal conductance–photosynthesis relationship. In detail, the prognostic equations of canopy and the soil surface energy balance take into account the heat storage terms of vegetation and surface soil layer. Also, a stomatal conductance scheme including a leaf water potential-related stress factor is used to update the popular stomatal conductance–photosynthesis models. The model parameters are calibrated with the multi-objective likelihood measure under the framework of Generalized Likelihood Uncertainty Estimation (GLUE), by which the parameter uncertainty and interactions between parameters and model responses are investigated.

## DESCRIPTION OF THE MODEL

The VIP model is designed to simulate the canopy carbon assimilation, radiation absorption, energy partitioning into heat fluxes and soil moisture and thermal dynamics. It consists of both vegetation and soil modules. In the vegetation module, canopy is divided into sunlit and shaded leave groups for energy partitioning and photosynthesis. In the soil module, soil moisture and thermal dynamics are described by Richards' equation considering thermal gradient induced water vapour flow, and the thermal diffusion equation for soil temperature, respectively.

**Prognostic equations**

The prognostic equations for energy balances at canopy and underneath soil surface are, respectively:

$$C_v \frac{\partial T_v}{\partial t} = R_{nv} - H_v - LE_v \tag{1}$$

$$C_{m1} \frac{\partial T_g}{\partial t} = R_{ng} - H_g - LE_g - G \tag{2}$$

where $C_v$ is the bulk heat capacity per unit area of canopy (J m$^{-2}$ K$^{-1}$), $C_{m1}$ is the bulk heat capacity per unit area of the upper soil layer (J m$^{-2}$ K$^{-1}$), $T_g$ and $T_v$ are the soil surface and canopy temperature (K) respectively, $L$ is the latent heat of evaporation (J kg$^{-1}$) and $G$ is the soil heat flux (W m$^{-2}$). $R_{nv}$ and $R_{ng}$ are the absorbed net radiation fluxes (W m$^{-2}$) by canopy and soil, $E_v$ and $E_g$ are vegetation transpiration (kg m$^{-2}$ s$^{-1}$) and soil evaporation (kg m$^{-2}$ s$^{-1}$) fluxes, respectively. $H_v$ and $H_g$ are sensible heat fluxes (W m$^{-2}$) from vegetation and soil, respectively.

The respective prognostic equations for soil moisture and thermal regimes are:

$$C_m \frac{\partial T_s}{\partial t} = \frac{\partial}{\partial z}(\lambda \frac{\partial T_s}{\partial z}) \tag{3}$$

$$\frac{\partial \vartheta}{\partial t} = \frac{\partial}{\partial z}[K_w(\frac{\partial \psi}{\partial z} + 1)] + \frac{\partial}{\partial z} D_T \frac{\partial T_s}{\partial z} - S_u(z,t) \tag{4}$$

where $C_m$ is the soil heat capacity (J m$^{-3}$ K$^{-1}$), $\lambda$ is the soil thermal conductivity (J m$^{-1}$ s$^{-1}$), $\vartheta$ is the soil moisture, $\psi$ is the soil water potential (m), $T_s$ is the soil temperature (K), $K_w$ is the soil hydraulic conductivity (m s$^{-1}$), $D_T$ is the diffusion coefficient for water vapour (m$^2$ s$^{-1}$ K$^{-1}$) in the soil, $S_u(z, t)$ is the sink term of root uptake (s$^{-1}$). Here $\psi$ and $K_w$ are parameterized with the Clapp & Hornberger (1978) equations using the parameter of saturated hydraulic conductivity, $K_{wsat}$ (m s$^{-1}$).

**Carbon flux**

The $CO_2$ flux ($F_c$, μmol m$^{-2}$ s$^{-1}$) above canopy is estimated as the sum of canopy net photosynthesis ($A_{nc}$), plant respiration ($R_{plant}$, μmol m$^{-2}$ s$^{-1}$) and soil respiration ($R_{soil}$, μmol m$^{-2}$ s$^{-1}$), namely:

$$F_c = A_{nc} - R_{plant} - R_{soil} \tag{5}$$

The canopy photosynthesis estimation is based on Farquhar's biochemical model (Farquhar *et al.*, 1980), in which the Rubisco capacity $V_{cmax}$ is assumed decreasing exponentially with cumulative leaf area index (LAI) from the top of canopy, namely:

$$V_{c\max} = V_{c\max 0} \exp(-K_N LAI) \tag{6}$$

where $V_{cmax0}$ is the value of $V_{cmax}$ at the canopy top, and $K_N$ is the extinction coefficient.

## Radiometric temperature

The canopy and ground surface temperature predicted by the model is chosen for calculation of the composite radiometric temperature, expressed as:

$$T_r = [\sigma_f \varepsilon_c T_v^4 + (1 - \sigma_f) \varepsilon_g T_g^4]^{1/4} \tag{7}$$

where $\varepsilon_c$ and $\varepsilon_g$ are the canopy and ground emissivities, respectively, set as 0.98 and 0.95, $\sigma_f$ is the canopy cover fraction, $T_r$ is the radiometric surface temperature (K) monitored by an infrared thermometer.

## Canopy conductance

Following Tuzet *et al.* (2003), we use the following relationship between stomatal conductance and carbon assimilation rate adopted, expressed as:

$$g_c = m \frac{A_{nc}}{c_s}(1 - \frac{\psi_v}{\psi_c}) \tag{8}$$

where $c_s$ is the CO₂ concentration at the leaf surface ($P_a$), $\psi_v$ is the leaf water potential (m), $m$ is an empirical coefficient. $\psi_c$ is the value of water potential at which total stomatal closure occurs, a value of $-250$ m is adopted (Federer, 1979).

The water flux from root zone to leaf, $J_w$ (kg m⁻² s⁻¹), is given by:

$$J_w = \rho_w \frac{\psi_s - \psi_v}{r_p + r_{hs}} \tag{9}$$

where $\rho_w$ is the water density (kg m⁻³), $\psi_s$ is the soil water potential in the root zone (m), $r_p$ is the plant hydraulic resistance (s), $r_{hs}$ is the soil hydraulic resistance (s). Under steady conditions, $J_w$ is equal to transpiration rate $E_v$.

## Wind profile and soil resistance for evaporation

For a horizontally homogeneous canopy, wind speed is assumed to decrease in the canopy as an exponential function:

$$u(z) = u(h_c) \exp(-w_e(1 - \frac{z}{h_c})) \tag{10}$$

where $u$ is the wind speed (s m⁻¹), $h_c$ is the canopy height (m), $w_e$ is the empirical coefficient, $z$ is the height above ground (m).

Soil resistance for water vapour diffusion from soil pores to the above near surface air is parameterized using the relationship of Sellers *et al.* (1992):

$$r_s = \exp(a_1 - b_1 \frac{\vartheta_1}{\vartheta_s}) \tag{11}$$

where $r_s$ is the soil resistance (m s⁻¹), $\vartheta_1$ and $\vartheta_s$ are the surface thin layer and the saturated moisture contents respectively, and $a_1$ and $b_1$ are the empirical coefficients.

## SITE AND DATA

The data were collected at a winter wheat field in Shunyi (SY, 116°33′E, 40°09′N), Beijing in 2001. The soil texture is silty loam with a granular structure. Total soil organic carbon concentration is 0.36% and dry bulk density of the root layer is about 1.3 g cm$^{-3}$.

The observation site is flat with a fetch more than 500 m. Microclimate variables of wind speed, and wet and dry bulb temperatures at 1 and 2 m above the ground were scanned every 15 s and output as 5 min averages with resolutions of 0.1 m s$^{-1}$ for wind speed and 0.1 K for air temperature, respectively. Global and reflected shortwave radiation, net radiation and soil heat fluxes were also measured. Radiometric surface temperature above 2 m of the canopy was measured with 45°-inclination angle by an infrared thermometer. Resolution of the infrared thermometer is 0.1 K. Turbulent fluxes of $CO_2$, latent and sensible heat fluxes were measured by the eddy covariance technique, in which $CO_2$ and water vapour fluxes were gathered with an open-path $CO_2/H_2O$ gas analyzer (Li-7500, LI-COR, USA). Wind and temperature variances were also gathered at the same height by the sonic anemometer (DA600, Kaijo, Japan) at a 20 Hz sampling rate.

## MULTI-OBJECTIVE LIKELIHOOD AND THE PRIOR PARAMETER RANGES

### Multi-objective likelihood

Multi-objective calibration is based on the minimization of a set of model performance fitness criteria in which each one corresponds to a model output variable. The measurements of $CO_2$, heat flux, surface temperature, soil moisture and surface albedo can be used to constrain the parameter values based on the multi-objective approach theory. In this case, 13 parameters are conditioned with five model responses against observations under the framework of GLUE methodology (Beven & Binley, 1992). The five variables are $CO_2$ flux, latent, sensible and soil heat fluxes, as well as infrared radiometric surface temperature, respectively. The agreement index ($R^2$, Willmott, 1981) is employed as an objective function for model performance evaluation and the likelihood measure for GLUE analysis:

$$L(Y \mid \zeta) \propto R^2 = \frac{\sum_{i=1}^{N}(Y_i - O_i)^2}{\sum_{i=1}^{N}(\mid Y_i - \overline{Y} \mid + \mid O_i - \overline{O} \mid)^2} \tag{12}$$

where $Y$ is the predicted variable, $\zeta$ is the parameter set, and $O$ is the observed variable. The average is noted with an over bar.

The likelihood measure including all single variable likelihood measure is updated using the Bayesian equation as:

$$L(\zeta \mid Y) = \prod_{i=5} L_i(Y \mid \zeta) / C \tag{13}$$

where $L_i$ ($i = 1, 5$) are the likelihood measures of the $CO_2$ flux, latent, sensible and soil heat fluxes, infrared radiometric surface temperature, respectively, and $C$ is the scaling factor.

**Table 1** Model input parameters sampled for Monte–Carlo simulations.

| Parameter | Definition | *Priori* range |
|---|---|---|
| $V_{cmax}$ | Carboxylation rate limited by Rubisco activity ($\mu$mol C m$^{-2}$s$^{-1}$) | 10–110 |
| $m$ | Coefficient of stomatal conductance / photosynthesis relationship | 2–14 |
| $\alpha$ | Quantum efficiency ($\mu$mol C/$\mu$mol photon) | 0.05–0.5 |
| $K_N$ | Extinction coefficient of leaf nitrogen in the canopy | 0.1–1.5 |
| $\lambda_s$ | Thermal conductivity of soil solid (J m$^{-1}$ s$^{-1}$) | $5 \times 10^{-6}$–$150 \times 10^{-6}$ |
| $K_{wsat}$ | Saturated soil hydraulic conductivity (m s$^{-1}$) | 0.05–2.0 |
| $r_p$ | Plant hydraulic resistance (s) | $0.5 \times 10^{8}$–$50 \times 10^{8}$ |
| $C_{hs}$ | Heat capacity of soil solid (J kg$^{-1}$) | 400–1200 |
| $z_{os}$ | Roughness of soil surface (m) | 0.001–0.01 |
| $c_r$ | Coefficient of root profile | 0.1–3 |
| $w_e$ | Wind speed extinction coefficient in the canopy | 0.5–4 |
| $a_1$ | Coefficient of the soil resistance for water vapour diffusion | 4–12 |
| $b_1$ | Coefficient of the soil resistance for water vapour diffusion | 2–6 |

## Parameters selected for sensitivity analysis

Thirteen main parameters, related to the processes of photosynthesis and available energy partitioning into sensible and latent heat fluxes, are selected: seven related to vegetation and six related to soil heat and moisture. These parameters are also closely related to the CO₂ flux and turbulent fluxes directly or indirectly, and are shown in Table 1. Ranges of the parameter values varied in the Monte Carlo sampling procedure in GLUE are also listed in Table 1.

Prior ranges of the selected parameter values are given according to their possible spaces, which are set a bit wider in this study than those found in the literature. Random sets of parameters (60 000) were sampled from uniform distributions across the specified ranges.

## RESULTS

### Model performance with multi-objective conditioning

The model performances are shown in Table 2, in which 524 parameter sets from 60 000 are selected as behaviours (0.9%). The agreement of net radiation with observations (not shown in Table 2) is the most satisfactory with RMSE of 13 W m$^{-2}$ relative to LE and H. The best fit $R^2$ values for surface temperature are as high as 0.99. The RMSE values are similar for both latent and sensible heat fluxes, whereas RMSE of ground heat flux is higher. The RMSE of soil heat flux is close to the deviation of energy budget (46 W m$^{-2}$). From the observations of ground heat flux, it can be seen that the values of $G$ measured by heat plates buried under the crop row and inter-row were noticeably different during the daytime, which is probably the main reason resulting in the deviation of the energy budget closure. Generally, the performance of our model, with $R^2$ values being greater than 0.8, is quite satisfactory, which is comparable with other models' efficiency (e.g. Leuning *et al*., 1998; Anderson *et al*., 2000; Zhan & Kustas, 2001; Arora, 2003; Ogee *et al*., 2003).

**Table 2** Model performances of the best fit for SY data set.

| | $F_C$ $R^2$ | RMSE ($\mu$mol $CO_2$ $m^{-2}$ $s^{-1}$) | $LE$ $R^2$ | RMSE (W $m^{-2}$) | $H$ $R^2$ | RMSE (W $m^{-2}$) | $G$ $R^2$ | RMSE W $m^{-2}$ | $T_r$ $R^2$ | RMSE (K) |
|---|---|---|---|---|---|---|---|---|---|---|
| Best fit | 0.97 | 2.3 | 0.94 | 34 | 0.96 | 24 | 0.82 | 52 | 0.99 | 2.2 |
| Behaviours | 0.90 | 3.5 | 0.90 | 43 | 0.93 | 33 | 0.79 | 66 | 0.97 | 3.1 |

## Multiple variables conditioning and equifinality

Scatter plots of the 13 parameters with likelihood measure, which can be regarded as projections of high dimensional parameter space onto a single axis, are presented in Fig. 1. It can be seen from the scatter plots that the better fits to the model response are presented in a wide range of the parameter space, even for the most sensitive parameters. This reinforces the concept of equifinality of model parameter sets in producing behavioural simulations in general view.

More than four parameters are significantly constrained and the behavioural values are aggregated around a certain zone in the prior set space. In detail, $V_{cmax}$ with the top likelihood measures is about 90 $\mu$mol $CO_2$ $m^{-2}$ $s^{-1}$ which is in agreement with the documented measured value for winter wheat as 93 $\mu$mol $m^{-2}$ $s^{-1}$ (used by S. B Verma's group, cited by Arora, 2003). The best-fit value of parameter $m$ is around 8. Leaf nitrogen content extinction coefficient in canopy $K_N$ is at the value of 0.5, near the field observed value of 0.43 reported by Dreccer *et al.* (2000). $\lambda_s$ is directly related with ground heat flux and the best fit values are located around the left side with a sharp pattern in the posterior range. However, the parameters $\alpha$, $w_e$, $r_p$, $K_{wsat}$, $C_{hs}$, $C_r$, $z_{os}$, $a_1$ and $b_1$ are not noticeably constrained by the observations.

## Interactions and compensations of the parameters

Generally, as pointed by Beven (2000), in a physically process-based model, the parameters should be specified theoretically. However, due to model structure and data availability, as an alternative, the specification of parameters relies on calibration or empirical relationships. So the calibrated parameter values are related to the model physical structure and errors in forcing data and measurement. As a consequence, they may be less physically "correct" with high correlation coefficients between parameters.

Calculating a linear Pearson correlation coefficient can most easily test the interactions and compensations between parameters. A Spearman rank correlation coefficient can additionally be used to test for nonlinear relationships (e.g. Wagener & Wheater, 2005). The significant values of correlation coefficient between parameters mean that the two relevant parameter values are compensating for each other to some extent during the calibrating process. Generally, neither a linear (Table 3(a)) nor a nonlinear (Table 3(b)) relationship exists between parameters with about 5.1~7.7% of 78 coefficient values being only larger than or equal to 0.2 (the bold values), indicating that the interactions and compensations between parameters are weak.
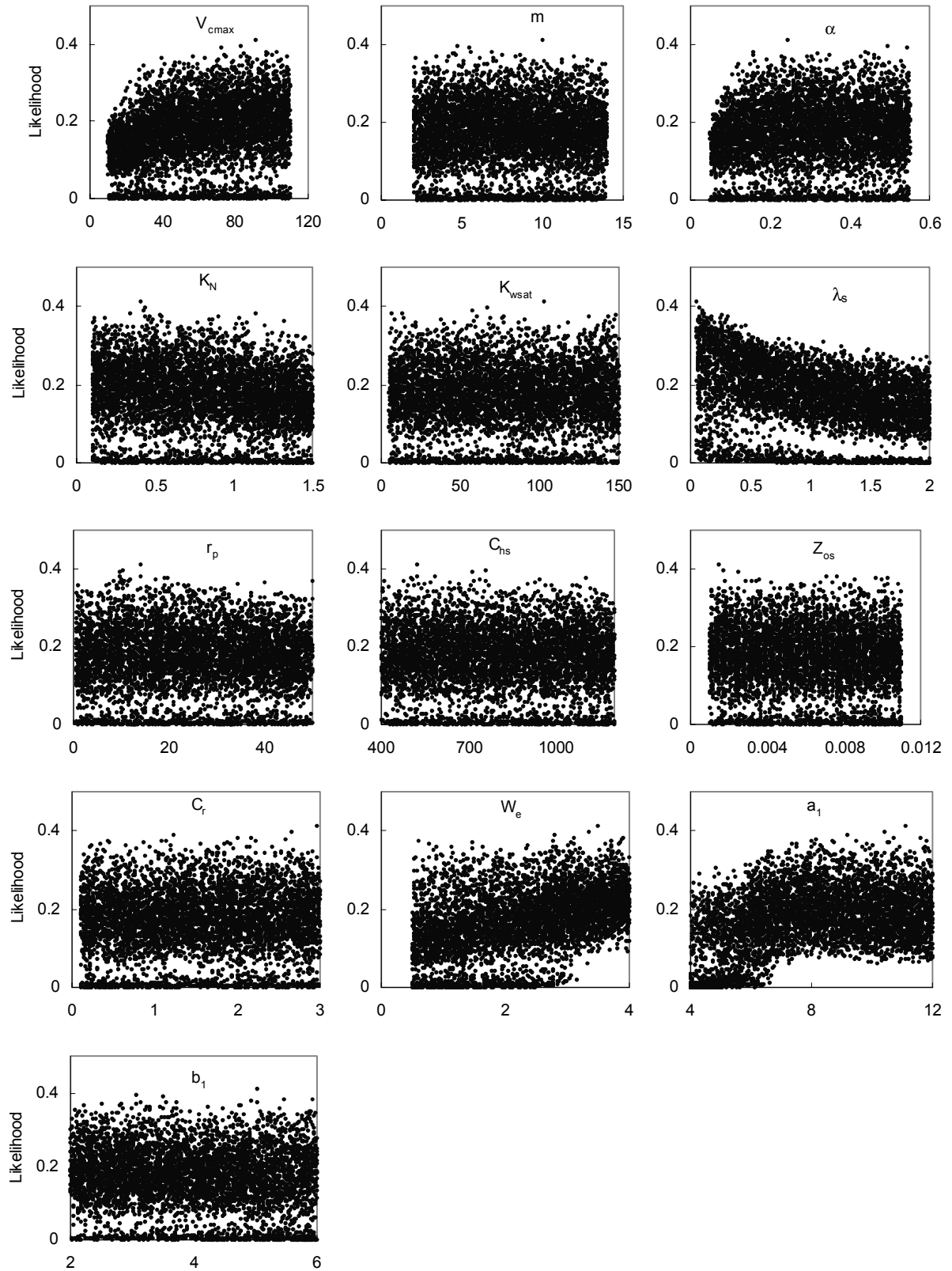
**Fig. 1** Scatter plots of the 13 parameters with likelihood measures at SY. The *x*-axis is the range of parameter and *y*-axis is the normalized likelihood.

**Table 3** Correlation coefficients of the 13 selected parameters derived from the behavioral values.

| | $V_{cmax}$ | $m$ | $\alpha$ | $K_N$ | $K_{wsat}$ | $\lambda_s$ | $r_p$ | $C_{hs}$ | $z_{os}$ | $C_r$ | $w_e$ | $a_1$ | $b_1$ |
|---|---|---|---|---|---|---|---|---|---|---|---|---|---|
| (a) Pearson Correlation coefficients | | | | | | | | | | | | | |
| $V_{cmax}$ | 1 | −0.10 | −0.05 | **0.42** | 0.00 | 0.00 | −0.12 | −0.08 | −0.04 | 0.02 | 0.01 | 0.11 | 0.06 |
| $m$ | | 1 | −0.11 | 0.16 | 0.04 | 0.03 | 0.07 | 0.04 | −0.04 | 0.06 | −0.01 | 0.06 | −0.07 |
| $\alpha$ | | | 1 | **0.24** | −0.02 | −0.03 | 0.01 | 0.02 | 0.02 | −0.11 | 0.02 | 0.02 | 0.00 |
| $K_N$ | | | | 1 | 0.01 | −0.15 | −0.03 | −0.04 | −0.02 | −0.09 | −0.04 | 0.04 | 0.00 |
| $K_{wsat}$ | | | | | 1 | 0.01 | −0.12 | 0.00 | 0.06 | −0.02 | 0.00 | 0.08 | 0.06 |
| $\lambda_s$ | | | | | | 1 | **−0.20** | −0.01 | −0.03 | −0.06 | 0.14 | −0.13 | 0.03 |
| $r_p$ | | | | | | | 1 | 0.05 | 0.01 | −0.05 | −0.17 | **−0.30** | 0.09 |
| $C_{hs}$ | | | | | | | | 1 | −0.02 | −0.04 | −0.01 | −0.01 | −0.02 |
| $z_{os}$ | | | | | | | | | 1 | −0.02 | 0.00 | 0.04 | 0.00 |
| $C_r$ | | | | | | | | | | 1 | −0.03 | 0.00 | 0.02 |
| $w_e$ | | | | | | | | | | | 1 | −0.10 | −0.02 |
| $a_1$ | | | | | | | | | | | | 1 | 0.03 |
| $b_1$ | | | | | | | | | | | | | 1 |
| (b) Spearman Rank correlation coefficients | | | | | | | | | | | | | |
| $V_{cmax}$ | 1 | −0.09 | −0.03 | **0.46** | 0.06 | 0.00 | −0.13 | 0.00 | −0.03 | −0.03 | −0.12 | 0.05 | −0.03 |
| $m$ | | 1 | −0.17 | 0.15 | −0.04 | −0.09 | 0.10 | 0.06 | −0.01 | 0.00 | −0.01 | **0.23** | −0.04 |
| $\alpha$ | | | 1 | **0.26** | 0.02 | 0.01 | −0.13 | −0.07 | 0.01 | −0.01 | 0.01 | 0.12 | 0.02 |
| $K_N$ | | | | 1 | 0.05 | −0.09 | −0.10 | −0.02 | −0.03 | −0.02 | 0.04 | 0.04 | 0.00 |
| $K_{wsat}$ | | | | | 1 | 0.03 | 0.01 | −0.01 | 0.04 | −0.02 | −0.01 | −0.05 | 0.08 |
| $\lambda_s$ | | | | | | 1 | −0.08 | −0.01 | −0.03 | 0.03 | 0.11 | −0.02 | 0.06 |
| $r_p$ | | | | | | | 1 | 0.03 | 0.00 | −0.03 | **0.22** | **−0.34** | 0.09 |
| $C_{hs}$ | | | | | | | | 1 | 0.05 | 0.03 | 0.05 | 0.08 | 0.03 |
| $z_{os}$ | | | | | | | | | 1 | 0.02 | 0.00 | 0.02 | 0.01 |
| $C_r$ | | | | | | | | | | 1 | 0.05 | −0.01 | −0.02 |
| $w_e$ | | | | | | | | | | | 1 | **−0.20** | 0.07 |
| $a_1$ | | | | | | | | | | | | 1 | 0.09 |
| $b_1$ | | | | | | | | | | | | | 1 |

A slightly stronger correlation was found between parameter $V_{cmax}$ and $K_N$ with correlation coefficient of 0.46, being the only one over 0.4. From model running experiences we know that the sensitivities of parameters to the different model responses are different. Parameters $V_{cmax}$ and $K_N$ are more sensitive to $CO_2$ flux, whereas most of the other parameters are more sensitive to heat fluxes, hence for parameters belonging to the same group, the compensation and interaction will be expected to be more significant.

There is no obvious difference between correlation coefficients and Spearman rank correlation coefficients. A slightly stronger nonlinear dependence than linear dependence occurs in two parameter pairs, $a_1 \sim w_e$ and $a_1 \sim m$, with the rank correlation coefficient being significantly larger than the linear correlation coefficient. However these relationships shows the significant interactions of energy exchanges between the canopy air space and underneath soil surface.

From the above correlation analysis, it seems that the interaction and compensation between parameters are not very obvious.

## Sensitivity analysis

Correlation analysis on the resulting data set can be used to identify the sensitivity of the output variable to the model parameters. If a parameter is highly correlated with the output variable of interest, then the output is sensitive to this parameter. However, neither the Pearson correlation coefficient nor the Spearman Rank correlation, coefficient as mentioned above, can clearly identify the sensitivity of output to the model parameters if the number of the parameters is larger than one. The reason is that multiple parameters affect the output simultaneously. The partial correlation coefficient (PCC) quantifies the amount of residual variation accounted for by individual parameter variation after the effects of all other parameters have been statistically removed (Saltelli *et al.*, 2000; Levy & Mackay, 2003), and hence is used here as the sensitivity index.

The PCC between the parameter and the combined likelihood $L$ are shown in Table 4. The order of the significance of the sensitivity of the model response to the parameters are as following: $a_1 > w_e > \lambda_s > V_{cmax} > K_N > b_1$. For those parameters, such as α, $r_p$, $K_{wsat}$, $z_{os}$, $C_{hs}$, $m$ and $C_r$, the sensitivity is quite insignificant as the PCCs are all $< 0.3$. The results on $\lambda_s$, $V_{cmax}$ and $K_N$ are in agreement with the scatter plots (Fig. 1). As the sensitivities of parameters to the corresponding model responses are different, it is usually difficult to achieve an effective calibration for all the parameters with a traditional single objective function, confirming the necessity of multi-objective calibration.

**Table 4** Partial correlation coefficients (PCC) of the 13 selected parameters with the likelihood measure.

|  | $V_{cmax}$ | $m$ | α | $K_N$ | $K_{wsat}$ | $\lambda_s$ | $r_p$ | $C_{hs}$ | $z_{os}$ | $C_r$ | $w_e$ | $a_1$ | $b_1$ |
|---|---|---|---|---|---|---|---|---|---|---|---|---|---|
| PCC | 0.65 | 0.01 | 0.28 | 0.42 | 0.05 | 0.73 | 0.08 | 0.02 | 0.05 | 0 | 0.84 | 0.92 | 0.41 |

## Evaluation of multi-objective calibrations

The contribution of each variable to the multi-objective likelihood measure is different. For a single objective likelihood measure denoted by {}, it usually gives good calibrated results of the same model response variable; for example, {$H$} is good for model predicted sensible heat flux. Combinations of the objective likelihood measures show quite different Pearson correlation coefficients with the likelihood of the five variables presented in Fig. 2. The constraining effects of the five objectives are different. For single objective functions, surface radiometric temperature leads to the highest correlation coefficient with the 5-objective likelihood. For the 2-objective functions, {$H,T_r$} reaches the highest efficiency with the second and third being {$F_c,T_r$} and {$LE,T_r$}, respectively. The combinations of two or more fluxes as likelihood {$LE, H$} and {$LE, H, F_c$} give a noticeably poorer efficiency than that of one flux and temperature combination. Thus it can be concluded that combinations of flux and state variable are more efficient for parameter constraining.
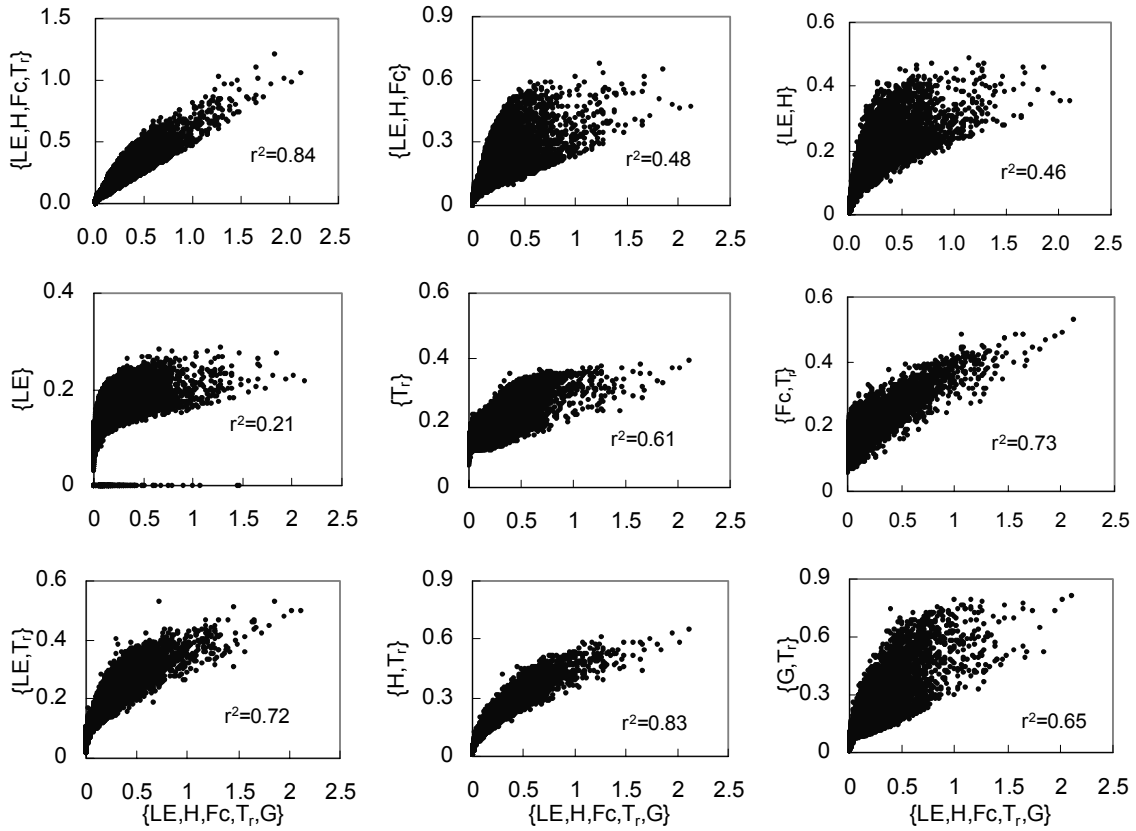
**Fig. 2** The correlation of the contributions of five variables to the multi-objective likelihood measure with the contributions of the different number of variables to the multi-objective likelihood measure.
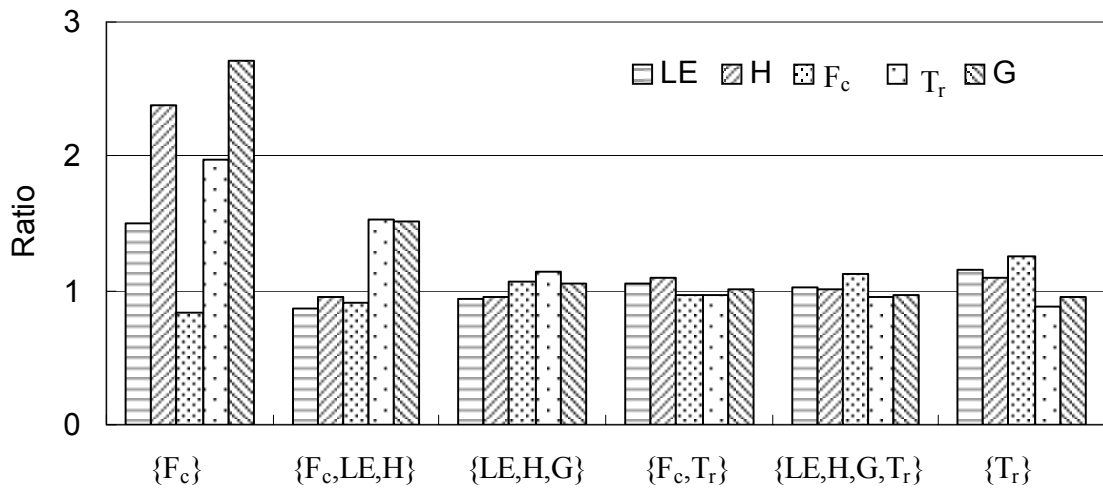


**Fig. 3** The ratios of RMSE by 1-, 2-, 3- and 4-objective likelihood measures to the 5-objective likelihood measure.

Figure 3 shows the ratios of RMSE by 1-, 2-, 3- and 4-objective likelihood measures to the 5-objective likelihood measure. The effects of {*LE, H, G*}, {*F$_c$, T$_r$*}, {*LE, H, G, T$_r$*} are close to the 5-objective likelihood measure {*LE, H, Fc, T*$_r$, *G*}. It is

easy to see that a multi-objective likelihood measure with one flux and one state variable can result in quite close effect to that with all the five objectives in this study. Gupta *et al.* (1999) also showed some similar results. The reason is that the state variables are more related to soil, vegetation heat and water capacities, whereas turbulent fluxes are more related to aerodynamic processes, giving rise to a higher calibration efficiency via combination of one flux and one state variable. On the other hand, the outstanding effect of surface radiometric temperature for calibration indicates that thermal remote sensing be a promising tool for distributed SVAT model calibration and evaluation over large areas.

## SUMMARY AND CONCLUSIONS

In this paper, the multi-objective technique under the framework of GLUE is chosen to assimilate the observed land surface fluxes and state variables for optimal multiple parameter specification and the parameters generality exploration for a SVAT model (VIP).

Agreement indexes of latent, sensible, ground heat and CO$_2$ fluxes and radiometric surface temperature between observed and model responses are used to calculate the multi-objective likelihood, in which 13 parameters are selected for calibration and evaluation of the model uncertainty. The results show that although a single objective effectively constrains the relevant model response, the multiple objectives including both fluxes and state variables do so more efficiently. The outstanding effect of surface radiometric temperature for calibration suggests that thermal remote sensing might be a promising tool for distributed SVAT model calibration and evaluation over large areas.

Using both the multivariate linear regression and nonlinear Spearman rank correlation analysis, it is shown that the VIP model also appears to have a serious equifinality problem similar to other SVAT models. However, the interaction and compensation effects of parameters are weak.

## REFERENCES

Anderson, M. C., Norman, J. M., Meyers, T. P. & Diak, G. R. (2000) Analytical model for estimating canopy transpiration and carbon assimilation fluxes based on canopy light-use efficiency. *Agric. For. Meteor.* **101**, 265–289.

Arora, V. K. (2003) Simulating energy and carbon fluxes over winter wheat using coupled land surface and terrestrial ecosystem models. *Agric. For. Meteor.* **118**, 21–47

Avissar, R. (1998) Which type of soil-vegetation-atmosphere transfer scheme is needed for general circulation models: a proposal for a. higher–order scheme. *J. Hydrol.* **212–213**, 136–154.

Beven, K. & Binley, A. (1992) The future of distributed models: model calibration and uncertainty prediction. *Hydrol. Processes* **6**, 279–298.

Clapp, R. B. & Hornberger, G. M. (1978) Empirical equations for some soil hydraulic properties. *Water Resour. Res.* **14**, 601–604.

Dreccer, M. F., Schapendonk, A. H. C. M., Slafer, G. A. & Rabbinge, R. (2000) Comparative response of wheat and oil seed rape to nitrogen supply: absorption and utilization efficiency of radiation and nitrogen during the reproductive stages determining yield. *Plant Soil* **220**, 189–205.

Farquhar, G. D., von Caemmerer, S. & Berry, J. A. (1980) A biochemical model of photosynthetic $CO_2$ assimilation in leaves of $C_3$ species. *Planta* **149**, 79–90.

Federer, C. A. (1979) A soil–plant–atmosphere model for transpiration and availability of soil moisture. *Water Resour. Res.* **15**, 555–562.

Franks, S. W. & Beven, K. J. (1999) Conditioning a multiple-patch SVAT model using uncertain time-space estimates of latent heat fluxes as inferred from remotely sensed data. *Water Resour. Res.* **35**, 2751–2761.

Grieb, T., Hudson, R. J. M, Shang, N., Spear, R. C., Gherini, S. A & Goldstein, R. A. (1999) Examination of model uncertainty and parameter interaction in a global carbon cycling model (GLOCO). *Environ. Int.* **25**(6/7), 787–803.

Gupta, H. V., Bastidas, L. A., Sorooshian, S. , Shuttleworth, W. J. & Yang, Z. L. (1999) Parameter estimation of a land surface scheme using multicriteria methods. *J. Geophys. Res.* **104**(D16), 19491–19503.

Leuning, R., Dunin, F. X & Wang, Y. （1998） A two-leaf model for canopy conductance, photosynthesis and partitioning of available. II. Comparison with measurements. *Agric. For. Meteor.* **91**, 113–125.

Levy, P. E. & McKay, H. M. (2003) Assessing tree seedling vitality tests using sensitivity analysis of a process-based growth model. *For. Ecol. Manage.* **183**(1–3), 77–93.

Mo, X. & Liu, S. (2001) Simulating evapotranspiration and photosynthesis of winter wheat over the growing season. *Agric. For. Meteor.* **109**, 203–222.

Mo, X. & Beven, K. (2004) Multi-objective parameter conditioning of a three-source wheat canopy model. *Agric. For. Meteor.* **122**, 39–63.

Ogee, J., Brunet, Y., Loustrau, D., Berbrigier, P. & Delzon, S. (2003) MuSICA, a $CO_2$, water and energy multiplayer, multileaf pine forest model: evaluation from hourly to yearly time scales and sensitivity analysis. *Glob. Change Biol.* **9**, 697–717.

Saltelli, A., Chan, K. & Scott, E. M. (2000) *Sensitivity Analysis*. Wiley, Chichester, UK.

Sellers, P. J., Berry, J. A., Collatz, G. J., Field, C. B. & Hall, F. G. (1992) Canopy reflectance, photosynthesis. *Remote Sens. Environ.* **42**, 187–216.

Tuzet, A., Perrier, A. & Leuning, R. (2003) A coupled model of stomatal conductance, photosynthesis and transpiration. *Plant, Cell Environ.* **26**, 1097–1116.

Wagener, T. & Wheater, H. S. (2005) Parameter estimation and regionalization for continuous rainfall-runoff models including uncertainty. *J. Hydrol.* Available online from http://www.sciencedirect.com/science/journal/00221694.

Willmott, C. J. (1981) On the validation of models. *Phys. Geogr.* **2**, 184–194.

Zhan, X. & Kustas, W. P. (2001) A coupled model of land surface $CO_2$ and energy fluxes using remote sensing data. *Agric. Forest Meteorol.* **107**, 131–152.